Hartikainen, Hannu; Tiitinen, Lauri; Laine, Sampo; Hinkkanen, Marko

Identification of mechanical impedance of an electric machine drive for drivetrain design

Published in:
2023 IEEE International Electric Machines and Drives Conference, IEMDC 2023

DOI:
10.1109/IEMDC55163.2023.10238992

Published: 15/05/2023

Document Version
Peer reviewed version

Identification of Mechanical Impedance of an Electric Machine Drive for Drivetrain Design

Hannu Hartikainen*, Lauri Tiitinen*, Sampo Laine†, and Marko Hinkkanen*
*Aalto University School of Electrical Engineering, Espoo, Finland
E-mail: hannu.1.hartikainen@aalto.fi; lauri.tiitinen@aalto.fi; marko.hinkkanen@aalto.fi
†Aalto University School of Engineering, Espoo, Finland
E-mail: sampo.laine@aalto.fi

***Abstract*—This paper proposes a method for identifying mechanical impedance of an electric machine drive for drivetrain design and analysis. The mechanical impedance describes the dynamics of an electric machine as seen from its mechanical terminals. It depends not only on the electric machine but also on the control system, which should be taken into account when analyzing torsional vibrations. If the black-box input-output time-domain models of the electric machine and its control system are available, the mechanical impedance can be extracted from simulations. The proposed identification method is based on signal injection in time-domain simulations. At steady-state operating points, an excitation signal is injected into the rotor speed and the response is observed in the electromagnetic torque. The method is validated by comparing the identified mechanical impedances with the corresponding analytical solutions.**

***Index Terms*—Electric machine drive, electromagnetic, electromechanical, identification, interaction, mechanical impedance, torsional vibrations.**

I. Introduction

Mechanical rotor systems of high-power and high-speed applications have to be carefully designed in order to avoid detrimental torsional vibrations. In electric machine drives, the mechanical system, the electromagnetic system, and the control system are interconnected, as illustrated in Fig. 1(a). The effects of the control system are often omitted in the design phase of a rotor system, which may in some cases increase the risk of torsional vibrations [1], [2]. The dynamics of an electric machine drive, as seen from its mechanical terminals, can be termed as *mechanical impedance* [3]. If the mechanical impedance is known in the drivetrain design phase, the risk of unexpected electromechanical interactions and torsional vibrations could be reduced.

There are several challenges in providing information on the mechanical impedance. The electric machine drives are nonlinear systems, and, therefore, their dynamics depend on the operating point. A control system can be quite complex, and control algorithms are not typically publicly available. Furthermore, the vibration analysis of rotor systems is typically carried out in the frequency domain, while the nonlinear drive dynamics are easiest to study in the time domain. It would be beneficial to be able to provide the mechanical impedance of an electric machine drive in a simple form that is compatible with the rotor system design practices. The concept of the mechanical impedance (or mechanical stiffness as its alternative representation) has been restricted to direct online machines [4]–[7], with some exceptions [8]. In the case of controlled drives, it is possible to derive analytical expressions for the mechanical impedance in some special cases [9]–[11], while it is difficult or impossible to analytically model more advanced control methods without oversimplification.

This paper proposes a method to extract the frequency response for the mechanical impedance from time-domain simulations by means of signal injection at steady-state operating points. An example machine model and control methods are selected such that analytical expressions are available for the resulting mechanical impedance, allowing the comparison of the identified and analytical results. The proposed method can be used for any high-fidelity machine models and control algorithms, if their black-box input-output time-domain models are available.

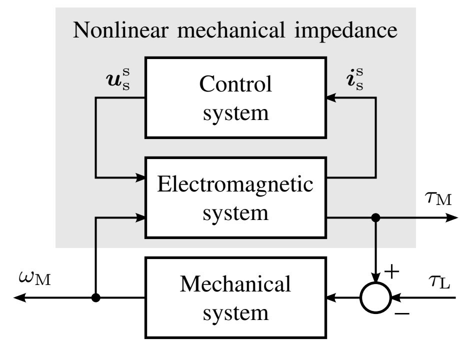

(a)

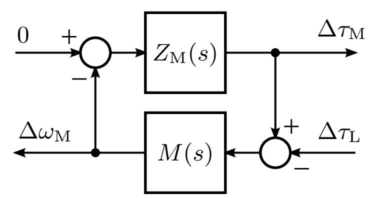

(b)

Fig. 1. Interconnection of the controlled electromagnetic system and the mechanical system: (a) nonlinear model; (b) linearized model. The transfer function $Z_\mathrm{M}(s)$ represents the mechanical impedance and the transfer function $M(s)$ represents the mechanical system (admittance). The example case in (a) assumes a motion-sensorless control system, but the approach can be extended to sensored drives as well.

II. Elements of Electromechanical Interaction

A. Mechanical Impedance

As already mentioned, the electric machine drive is a nonlinear system. In order to apply well-known linear analysis and design methods [12], the linearized drive dynamics are considered, as shown in Fig. 1(b). In an operating point of interest, the transfer function corresponding to the mechanical impedance is [3]

$$Z_\mathrm{M}(s) = -\frac{\Delta\tau_\mathrm{M}(s)}{\Delta\omega_\mathrm{M}(s)} \tag{1}$$

where ω_M is the mechanical angular speed of the rotor, τ_M is the electromagnetic torque, and Δ is used to mark the small-signal quantities. The negative sign in (1) is chosen in order to be able to use the standard negative feedback convention in the system interconnection [9], [13]. The mechanical impedance depends on the electromagnetic characteristics of the machine as well as on its control system, while it is independent of the mechanical system. If needed, the mechanical impedance can be easily translated to the mechanical stiffness [4], [5]

$$K_\mathrm{M}(s) = -\frac{\Delta\tau_\mathrm{M}(s)}{\Delta\vartheta_\mathrm{M}(s)} = sZ_\mathrm{M}(s) \tag{2}$$

where ϑ_M denotes the mechanical angle of the rotor.

B. Mechanical Admittance

The transfer function for the mechanical admittance (also known as mobility) is given by

$$M(s) = \frac{\Delta\omega_\mathrm{M}(s)}{\Delta\tau_\mathrm{M}(s)} \tag{3}$$

Even if mechanical systems are typically considered as linear systems, the small-signal notation is used here. While mechanical admittance models are not needed in the proposed identification method, they are exemplified below in order to provide the context.

In an ideal case of a rigid system, the mechanical admittance is

$$M(s) = \frac{1}{Js} \tag{4}$$

where J is the total moment of inertia of the electric machine and the mechanical load. Angular rotor vibrations may also occur in a rigid mechanical system if coupled with non-passive mechanical impedance [9].

In practice, rotor systems are never perfectly rigid. As an example, the mechanical point admittance of a two-mass system is [14]

$$M(s) = \frac{1}{Js}\frac{J_\mathrm{L}s^2 + C_\mathrm{S}s + K_\mathrm{S}}{(J_\mathrm{M}J_\mathrm{L}/J)s^2 + C_\mathrm{S}s + K_\mathrm{S}} \tag{5}$$

where J_M and J_L are the machine and load side inertias, respectively, $J = J_\mathrm{M} + J_\mathrm{L}$ is the total inertia, K_S is the torsional stiffness of the shaft, and C_S is the torsional viscous damping of the shaft. It is worth noticing that the torsional dynamics are not covered solely by the mechanical admittance, but the mechanical impedance affects them, especially in the first few torsional modes [7].

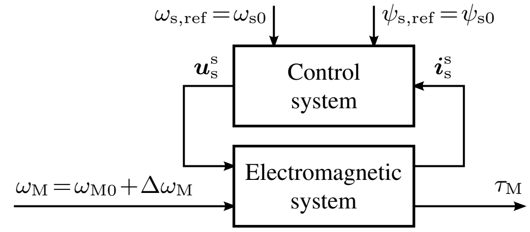

Fig. 2. Configuration of the simulation model in an identification process. In this example, the references for the control system correspond to V/Hz control of an induction machine.

C. Passivity

When analyzing the mechanical impedance $Z_\mathrm{M}(s)$ and the mechanical admittance $M(s)$, the notion of *passivity* is useful [9]–[11]. Passive systems are always stable, while the opposite is not generally true. Furthermore, the negative feedback interconnection (see Fig. 1) as well as the parallel interconnection of any passive systems is also passive [13], [15]. These features facilitate modular design and analysis of subsystems.

The mechanical impedance is used as an example system in the following definition. A precondition for a system to be passive is its stability, which always holds for the mechanical impedance $Z_\mathrm{M}(s)$ in open loop as well as with any feasible control system. The remaining passivity condition is [15]

$$\mathrm{Re}\{\boldsymbol{Z}_\mathrm{M}(\mathrm{j}\omega)\} \geq 0 \quad \text{for all } \omega \in [-\infty, \infty] \tag{6}$$

This condition equivalently means that the phase of $\boldsymbol{Z}_\mathrm{M}(\mathrm{j}\omega)$ is in the interval $[-90°, 90°]$ for all frequencies.

The mechanical admittances of most typical mechanical loads are passive, including the rigid system (4) and the two-mass system (5). On the other hand, electromagnetic systems in open loop tend to have non-passive operating regions [9]. By means of the control system, it is possible to passivate the mechanical impedance [10], [11], which makes the drive robust against unknown mechanical admittances.

III. Proposed Identification Method

The proposed identification method is based on signal injection at steady-state operating points in time-domain simulations. Fig. 2 shows an example configuration of the time-domain simulation model, where it is important to note that no mechanical system is used. The excitation signal $\Delta\omega_\mathrm{M}$ is injected into the rotor speed around the operating speed ω_M0, i.e., $\omega_\mathrm{M} = \omega_\mathrm{M0} + \Delta\omega_\mathrm{M}$.

In this paper, a sinusoidal excitation signal is considered,

$$\Delta\omega_\mathrm{M} = A\cos(\omega t) \tag{7}$$

where A is the amplitude of the excitation and ω is the excitation angular frequency, i.e., the angular frequency at which the mechanical impedance in (1) is to be evaluated for. The amplitude of the excitation signal should be low enough in order to not compromise the underlying small-signal assumption. Due to the properties of the mechanical impedance, it is advisable to increse the amplitude with

TABLE I
DATA OF THE 45-KW INDUCTION MACHINE

Nominal values	
Voltage (line-to-neutral, peak value)	$\sqrt{2/3} \cdot 400$ V
Current (peak value)	$\sqrt{2} \cdot 81$ A
Frequency	50 Hz
Speed	1477 r/min
Torque	291 Nm
Parameters	
Stator resistance R_s	60 mΩ
Rotor resistance R_R	30 mΩ
Leakage inductance L_σ	2.2 mH
Magnetizing inductance L_M	24.5 mH
Number of pole pairs n_p	2

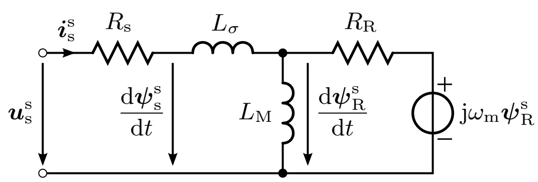

Fig. 3. Inverse-Γ equivalent circuit of an induction machine.

the excitation frequency, e.g., proportionally to the excitation frequency.

The benefit of using sinusoidal excitation is its high signal-to-noise ratio, which allows to use relatively low excitation amplitudes. Its drawback is that the frequency response can be extracted only for a single excitation frequency at a time, resulting in increased computing time. In order to expedite the identification procedure, the proposed method could be realized using wideband injection signals, such as a pseudo-random binary sequence [16].

Injecting a sinusoidal signal with an angular frequency of ω into the rotor speed induces a response to the electromagnetic torque with the same angular frequency. The electromagnetic torque phasor, corresponding to the excitation frequency ω, is obtained using the discrete Fourier transform [17]

$$\boldsymbol{\tau}_\mathrm{M}(\omega) = \frac{1}{N}\sum_{n=0}^{N-1} \tau_\mathrm{M}(n)\mathrm{e}^{-\mathrm{j}\omega n/N} \tag{8}$$

where n is the sample index and N is the number of samples. The rotor speed phasor $\boldsymbol{\omega}_\mathrm{M}$ is computed similarly. The frequency response of the mechanical impedance at the excitation frequency is then computed as

$$\boldsymbol{Z}_\mathrm{M}(\mathrm{j}\omega) = -\frac{\boldsymbol{\tau}_\mathrm{M}(\omega)}{\boldsymbol{\omega}_\mathrm{M}(\omega)} \tag{9}$$

All the other frequencies of interest are evaluated in the same manner.

IV. EXAMPLE MACHINE DRIVE SYSTEM

A 45-kW induction machine drive is used as an example system for the proposed identification method. The nominal values and parameters of the machine are given in Table I.

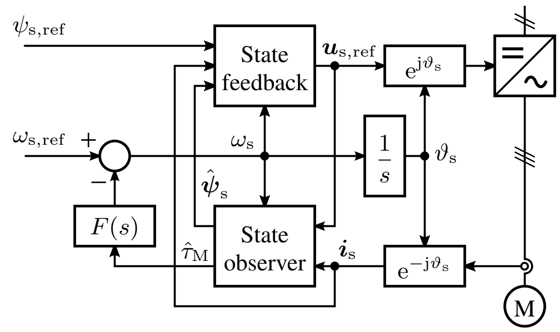

Fig. 4. Observer-based V/Hz control.

A. Induction Machine Model

The induction machine is modeled using the standard inverse-Γ model shown in Fig. 3. Complex space vectors are used, marked in boldface. In synchronous coordinates rotating at ω_s, the voltage equations are

$$\frac{\mathrm{d}\boldsymbol{\psi}_\mathrm{s}}{\mathrm{d}t} = \boldsymbol{u}_\mathrm{s} - R_\mathrm{s}\boldsymbol{i}_\mathrm{s} - \mathrm{j}\omega_\mathrm{s}\boldsymbol{\psi}_\mathrm{s} \tag{10a}$$
$$\frac{\mathrm{d}\boldsymbol{\psi}_\mathrm{R}}{\mathrm{d}t} = -R_\mathrm{R}\boldsymbol{i}_\mathrm{R} - \mathrm{j}\omega_\mathrm{r}\boldsymbol{\psi}_\mathrm{R} \tag{10b}$$

where $\boldsymbol{u}_\mathrm{s}$ is the stator voltage, $\boldsymbol{i}_\mathrm{s}$ is the stator current, R_s is the stator resistance, $\boldsymbol{i}_\mathrm{R}$ is the rotor current, R_R is the rotor resistance, $\omega_\mathrm{r} = \omega_\mathrm{s} - \omega_\mathrm{m}$ is the slip angular frequency, $\omega_\mathrm{m} = n_\mathrm{p}\omega_\mathrm{M}$ is the electrical angular speed of the rotor, and n_p is the number of pole pairs. The stator and rotor flux linkages, respectively, are given by

$$\boldsymbol{\psi}_\mathrm{s} = L_\sigma\boldsymbol{i}_\mathrm{s} + \boldsymbol{\psi}_\mathrm{R} \tag{10c}$$
$$\boldsymbol{\psi}_\mathrm{R} = L_\mathrm{M}(\boldsymbol{i}_\mathrm{s} + \boldsymbol{i}_\mathrm{R}) \tag{10d}$$

The electromagnetic torque is

$$\tau_\mathrm{M} = \frac{3n_\mathrm{p}}{2}\mathrm{Im}\{\boldsymbol{i}_\mathrm{s}\boldsymbol{\psi}_\mathrm{s}^*\} \tag{11}$$

where the superscript $*$ marks the complex conjugate.

B. Example Control Methods

Two example control schemes with known closed-form mechanical impedances are considered: open-loop V/Hz control [9] and observer-based V/Hz control [10]. In both methods, slip compensation is disabled and the stator flux reference is $\psi_\mathrm{s,ref} = 1$ p.u.

1) Open-Loop V/Hz Control: An open-loop V/Hz control algorithm can be expressed as

$$\frac{\mathrm{d}\vartheta_\mathrm{s}}{\mathrm{d}t} = \omega_\mathrm{s,ref} \tag{12a}$$
$$\boldsymbol{u}_\mathrm{s,ref} = R_\mathrm{s}\boldsymbol{i}_\mathrm{s,ref} + \mathrm{j}\omega_\mathrm{s,ref}\psi_\mathrm{s,ref} \tag{12b}$$
$$\boldsymbol{u}_\mathrm{s,ref}^\mathrm{s} = \boldsymbol{u}_\mathrm{s,ref}\mathrm{e}^{\mathrm{j}\vartheta_\mathrm{s}} \tag{12c}$$

where $\omega_\mathrm{s,ref}$ is the rate-limited stator angular frequency reference, ϑ_s is the angle for coordinate transformation, and $\boldsymbol{u}_\mathrm{s,ref}^\mathrm{s}$ is the voltage reference in stator coordinates. In the following, the stator resistance voltage drop (RI) compensation is omitted by setting $\boldsymbol{i}_\mathrm{s,ref} = 0$.

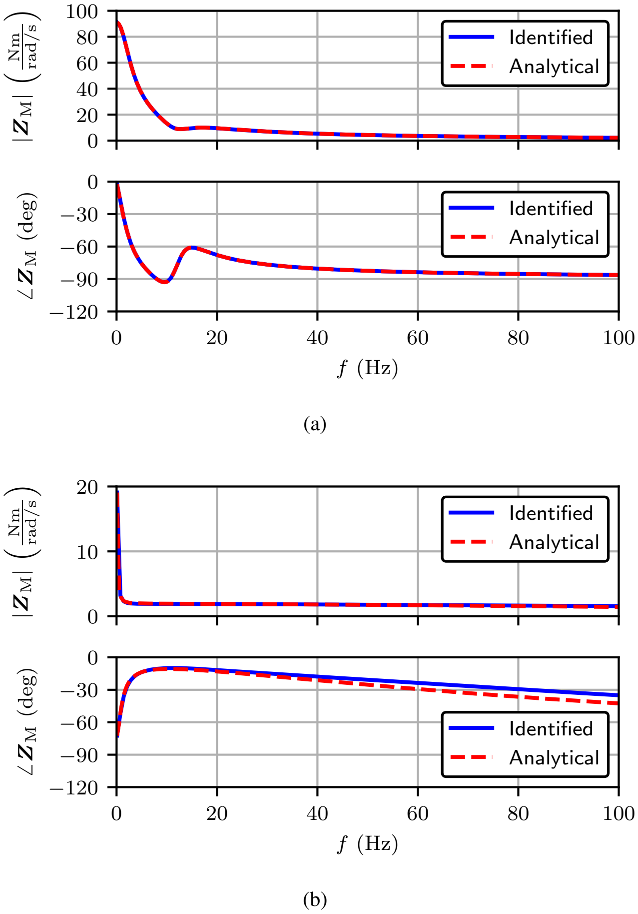

(a)

(b)

Fig. 5. Frequency response of the mechanical impedance at $\omega_{s0} = 0.25$ p.u. and $\tau_{M0} = 0$: (a) open-loop V/Hz control; (b) observer-based V/Hz control. The dashed red line shows the analytical frequency response and the solid blue line shows the identification result.

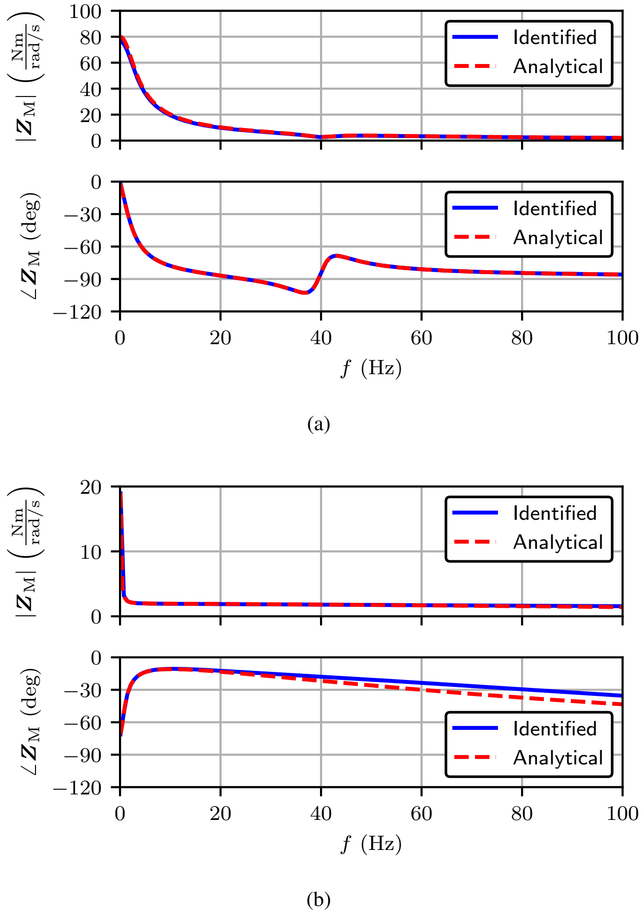

(a)

(b)

Fig. 6. Frequency response of the mechanical impedance at $\omega_{s0} = 0.8$ p.u. and $\tau_{M0} = 0.8$ p.u.: (a) open-loop V/Hz control; (b) observer-based V/Hz control. The dashed red line shows the analytical frequency response and the solid blue line shows the identification result.

The mechanical impedance of open-loop V/Hz control equals that of the induction machine alone since there is no feedback in the control. The analytical expression is available in [9].

2) Observer-Based V/Hz Control: Fig. 4 shows the block diagram of observer-based V/Hz control [10]. The voltage reference is calculated in synchronous coordinates as

$$\boldsymbol{u}_{\mathrm{s,ref}} = R_{\mathrm{s}}\boldsymbol{i}_{\mathrm{s}} + \mathrm{j}\omega_{\mathrm{s}}\psi_{\mathrm{s,ref}} + \alpha_{\mathrm{s}}(\psi_{\mathrm{s,ref}} - \hat{\boldsymbol{\psi}}_{\mathrm{s}}) \tag{13}$$

where $\hat{\boldsymbol{\psi}}_{\mathrm{s}}$ is the stator flux estimate provided by a sensorless flux observer and α_{s} is a state feedback gain, corresponding to the bandwidth of the closed-loop stator flux dynamics. The internal stator frequency reference is selected as

$$\omega_{\mathrm{s}} = \omega_{\mathrm{s,ref}} - \underbrace{\frac{k_\omega s}{s+\alpha_{\mathrm{f}}}}_{F(s)}\hat{\tau}_{\mathrm{M}} \tag{14}$$

where $\hat{\tau}_{\mathrm{M}}$ is a torque estimate given by the observer, k_ω is a positive gain, and $F(s)$ is a high-pass filter with bandwidth α_{f}. The feedback from the torque estimate is used to increase the damping of the system.

As shown in [10], the mechanical impedance resulting from observer-based V/Hz control can be expressed as

$$Z_{\mathrm{M}}(s) = \frac{N(s)}{(R_{\mathrm{R}}/\psi_{\mathrm{R0}}^2)\left[(s+\omega_{\mathrm{rb}})^2+\omega_{\mathrm{r0}}^2\right] + F(s)N(s)} \tag{15}$$

where ω_{rb} is the breakdown slip frequency, $\omega_{\mathrm{r0}} = \omega_{\mathrm{s0}} - \omega_{\mathrm{m0}}$ is the operating point slip-frequency, ψ_{R0} is the rotor flux magnitude at the operating point, and the numerator polynomial is $N(s) = \omega_{\mathrm{rb}}s + \omega_{\mathrm{rb}}^2 - \omega_{\mathrm{r0}}^2$. Naturally, the corresponding frequency response at the excitation angular frequency ω is obtained by substituting $s = \mathrm{j}\omega$. This mechanical impedance is passive in the whole feasible operating region.

The following parameters are used: state-feedback gain $\alpha_{\mathrm{s}} = 2\pi\cdot 20$ rad/s; high-pass filter bandwidth $\alpha_{\mathrm{f}} = 2\pi\cdot 1$ rad/s; and the damping gain $k_\omega = 0.5\ (\mathrm{Nm}\cdot\mathrm{s})^{-1}$. The observer bandwidth is set to $2\pi\cdot 40$ rad/s.

V. Results

The frequency response of the mechanical impedance is identified for the 45-kW induction machine for both open-loop V/Hz and observer-based V/Hz control. In the time-domain simulations, pulse-width modulation is omitted, the inverter

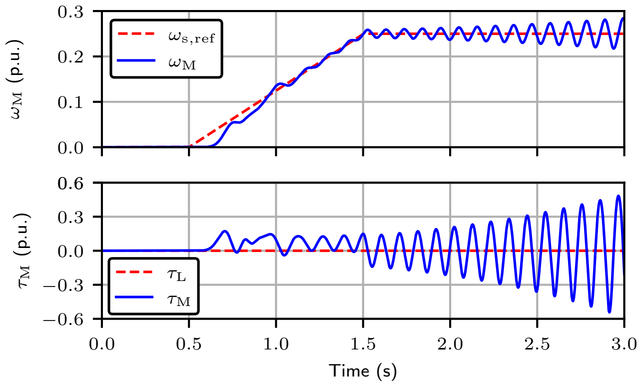

(a)

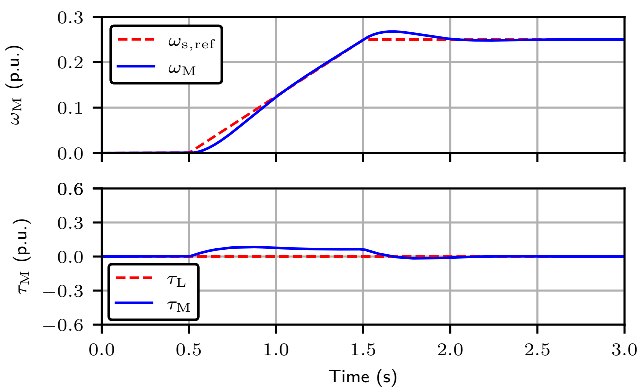

(b)

Fig. 7. Simulation results showing acceleration from zero speed to the speed of 0.25 p.u. in no-load condition: (a) open-loop V/Hz control; (b) observer-based V/Hz control.

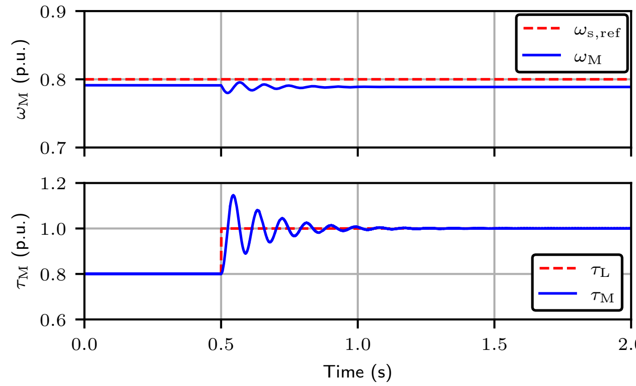

(a)

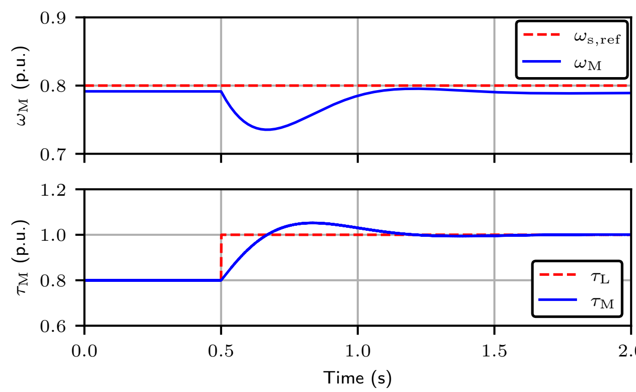

(b)

Fig. 8. Simulation results for a load torque step at the stator frequency of 0.8 p.u.: (a) open-loop V/Hz control; (b) observer-based V/Hz control.

is assumed to be lossless, and the DC-bus voltage is 540 V. The control system operates in discrete time with a sampling frequency of 4 kHz. The computational delay of one sampling period is modeled. The induction machine and mechanical system are modeled in continuous time. The identification method is implemented at the open-source machine drive simulation platform [18].

A. Identified Mechanical Impedance

The mechanical impedances resulting from both open-loop and observer-based V/Hz control methods are identified at two different operating points. The rotor speed and electromagnetic torque are sampled at the rate of 80 kHz for the discrete Fourier transform. The identified frequency response has a resolution of 150 linearly spaced samples for frequencies from 0.1 Hz to 100 Hz.

1) Lower Speed at No Load: Fig. 5 shows the mechanical impedance at the stator angular frequency $\omega_{\mathrm{s0}} = 0.25$ p.u. and at no load ($\tau_{\mathrm{M0}} = 0$). Figs. 5(a) and (b) show the identification results for open-loop V/Hz control and for observer-based V/Hz control, respectively. The analytical solutions are also shown as references. It can be seen that the identified results agree very well with the analytical solutions. In the case of observer-based V/Hz control, the identified impedance differs slightly from the analytical solution (15) at higher frequencies. This discrepancy originates from the discrete-time implementation of the controller, which is not considered in the analytical solution.

In the case of open-loop V/Hz control [Fig. 5(a)], the phase of the mechanical impedance goes below $-90°$ around the frequency of 10 Hz, indicating non-passive mechanical impedance at this operating point. Instead of dissipating the energy from torsional vibrations, this negative damping at some frequencies could increase the vibrations, thus introducing the risk of instability. On the other hand, in the case of observer-based V/Hz control [Fig. 5(b)], the phase remains between $-90°$ and $90°$ at all frequencies. As expected, the control system passivates the mechanical impedance in this case. Consequently, the drive system is stable with any passive mechanical system.

2) Higher Speed Under Load: Fig. 6 shows identified mechanical impedance at the stator angular frequency $\omega_{\mathrm{s0}} = 0.8$ p.u. and at the electromagnetic torque $\tau_{\mathrm{M0}} = 0.8$ p.u. Figs. 6(a) and (b) show the results for open-loop V/Hz control and for observer-based V/Hz control, respectively. It can be seen that the shape of the frequency response in the case of open-loop V/Hz control is similar to the operating point at the lower speed [Fig. 5(a)], but the frequency response is shifted due to the change in the operating-point stator frequency. On the other hand, in the case of observer-based V/Hz control, the analytical mechanical impedance is almost independent of the operating point, as could be expected based on (15). In both cases, the identified mechanical impedances match very well with the analytical ones. It can also be noticed that the mechanical impedance of open-loop V/Hz control is non-passive also at this operating point (the phase is below $-90°$ in the frequency range 25…40 Hz), while observer-based V/Hz control is passive.

B. Time-Domain Simulations

To showcase the interaction of the mechanical impedance and the mechanical admittance, two different time-domain simulation sequences are considered. In both sequences, The rigid mechanics in (4) with the total moment of inertia $J = 0.49\ \mathrm{kgm}^2$ are assumed.

1) Acceleration at No Load: Fig. 7 shows the simulation sequence, in which the stator frequency reference $\omega_{\mathrm{s,ref}}$ is ramped from zero to 0.25 p.u. and the load torque is zero. Figs. 7(a) and (b) show the results for open-loop V/Hz control and observer-based V/Hz control, respectively. After the acceleration, the operating point corresponds to that used in the mechanical impedance analysis in Fig. 5.

It can be seen that open-loop V/Hz control becomes unstable, which can be expected based on the stability analysis provided in [9]. Furthermore, the risk of the instability is predicted by the non-passive mechanical impedance, as explained earlier. In general, the stability of open-loop V/Hz control depends on the machine parameters and the mechanical system. In this example case, a sufficient increase of the inertia would stabilize the drive system. On the other hand, observer-based V/Hz control is stable, as expected based on its passive mechanical impedance.

2) Load Torque Step: The load torque step response is indirectly related to the mechanical impedance. The load torque causes the rotor speed to change, which further affects the electromagnetic torque through the mechanical impedance.

Fig. 8 shows the load torque steps from 0.8 p.u. to 1 p.u., while the stator frequency reference is kept constant at 0.8 p.u. Hence, the initial operating point corresponds to that used in the mechanical impedance analysis in Fig. 6. Figs. 8(a) and (b) show the results for open-loop V/Hz control and observer-based V/Hz control, respectively. It can be observed that open-loop V/Hz control responds faster to the load change than observer-based V/Hz control, as could be predicted based on the corresponding mechanical impedances shown in Fig. 6.

VI. Conclusion

The concept of mechanical impedance effectively captures the dynamics of a controlled electric machine drive as seen from its mechanical terminals. The proposed identification method can be used to extract the frequency response of the mechanical impedance from time-domain simulations. The identified response can be used to predict the drivetrain stability and to prevent torsional vibrations. The proposed method is validated by comparing the identified mechanical impedances with the known analytical expressions.

References

[1] T. Holopainen, J. Niiranen, P. Jörg, and D. Andreo, "Electric motors and drives in torsional vibration analysis and design," in *Proc. 42nd Turbomachinery Symp.*, Houston, TX, USA, Oct. 2013.

[2] M. A. Corbo, "VFDs — the torsional analyst's best friend or worst enemy?" in *Proc. GMRC Gas Machinery Conf.*, Louisville, KY, USA, Oct. 2021.

[3] C. M. Harris and A. G. Piersol, *Harris' Shock and Vibration Handbook*, 5th ed. New York, USA: McGrawn-Hill, 2002.

[4] I. M. Canay, "A novel approach to the torsional interaction and electrical damping of the synchronous machine, part I: Theory," *IEEE Trans. Power App. Syst.*, vol. PAS-101, no. 10, pp. 3630–3638, Oct. 1982.

[5] A. Tabesh and R. Iravani, "Frequency-response analysis of torsional dynamics," *IEEE Trans. Power Syst.*, vol. 19, no. 3, pp. 1430–1437, Aug. 2004.

[6] T. Holopainen, A.-K. Repo, and J. Järvinen, "Electromechanical interaction in torsional vibrations of drive train systems including an electrical machine," in *Proc. IFToMM Int. Conf. Rotordynamics*, Seoul, Korea, Sep. 2010, pp. 933–940.

[7] T. Holopainen and A. Arkkio, "Simple electromagnetic motor model for torsional analysis of variable speed drives with an induction motor," *Technische Mechanik*, vol. 37, no. 2-5, pp. 347–357, Jun. 2017.

[8] L. Harnefors, "Analysis of subsynchronous torsional interaction with power electronic converters," *IEEE Trans. Power Syst.*, vol. 22, no. 1, pp. 305–313, Feb. 2007.

[9] M. Hinkkanen, L. Tiitinen, E. Mölsä, and L. Harnefors, "On the stability of volts-per-hertz control for induction motors," *IEEE J. Emerg. Sel. Topics Power Electron.*, vol. 10, no. 2, pp. 1609–1618, Apr. 2022.

[10] L. Tiitinen, M. Hinkkanen, and L. Harnefors, "Stable and passive observer-based V/Hz control for induction motors," in *Proc. IEEE Energy Convers. Congr. Expo.*, Detroit, MI, USA, Oct. 2022.

[11] L. Tiitinen, M. Hinkkanen, J. Kukkola, M. Routimo, G. Pellegrino, and L. Harnefors, "Stable and passive observer-based V/Hz control for synchronous motors," in *Proc. IEEE Energy Convers. Congr. Expo.*, Detroit, MI, USA, Oct. 2022.

[12] G. F. Franklin, J. D. Powell, and A. Emami-Naeini, *Feedback Control of Dynamic Systems*, 5th ed. Upper Saddle River, NJ, USA: Prentice-Hall, 2006.

[13] F. Zhu, M. Xia, and P. J. Antsaklis, "Passivity analysis and passivation of feedback systems using passivity indices," in *Proc. American Control Conf.*, Jun. 2014, pp. 1833–1838.

[14] S. E. Saarakkala and M. Hinkkanen, "Identification of two-mass mechanical systems using torque excitation: Design and experimental evaluation," *IEEE Trans. Ind. Appl.*, vol. 51, no. 5, pp. 4180–4189, Sep./Oct. 2015.

[15] H. K. Khalil, *Nonlinear Systems*, 2nd ed. Upper Saddle River, NJ: Prentice-Hall, 1996.

[16] L. Ljung, *System Identification: Theory for the User*, 2nd ed. New York, USA: Prentice-Hall, 1999.

[17] J. G. Proakis and D. K. Manolakis, *Digital Signal Processing*, 4th ed. Upper Saddle River, NJ, USA: Prentice-Hall, 2006.

[18] L. Tiitinen, H. Hartikainen, L. Peretti, and M. Hinkkanen, "*motulator*: Motor drive simulator in Python," in *Proc. IEEE IEMDC*, San Francisco, CA, USA, May 2023.